The development of molecular tools for investigating NAD+ metabolism and signalling

Minnee, H.

Chapter 7

Summary and future prospects

Protein function, localization and processing are tightly regulated through a wide array of chemical alterations that are collectively referred to as post-translational modifications (PTMs). Nicotinamide adenine dinucleotide (NAD^+) is the substrate used for the introduction of the ubiquitous and highly dynamic PTM in which either one or multiple adenosine diphosphate ribose (ADPr) moieties are covalently attached to a nucleophilic side chain of an specific amino acid in the target protein. Such modification is termed mono-ADP-ribosylation (MARylation) if only a single ADPr-moiety is attached to the protein and referred to as poly-ADP-ribosylation (PARylation) when a number of ADPr-residues form linear or branched structures at the site of the modification. A variety of molecular tools, including well-defined ADPr oligomers, ADP-ribosylated oligopeptides and fluorogenic ADPr analogues, have been developed to elucidate the underlying mechanisms of ADP-ribosylation. A comprehensive overview of the ADPr-toolbox has been recently provided by Van der Heden van Noort,[1] while Liu *et al.* reviewed the synthetic methods towards oligo-ADPr-chains and ADPr peptides in more detail.[2] Since then, new insights in the variety of ADPr acceptor sites have sparked interest in the synthesis of mono-ADP-ribosylated peptides, carrying the ADPr moiety on different amino acid residues, which subsequently have been used to unravel the role of these modifications in ADPr-biology. Accordingly, an in-depth and up-to-date review on the chemoenzymatic and chemical methodologies to assemble peptides modified with a single ADPr moiety, connected via either native or artificial linkages to the peptides, is presented in **Chapter 1**.

The ADP-ribosylation of histidine has been observed in mass-spectrometry (MS)-based proteomic experiments. Lacking any structural information, there are two potential modification sites in the imidazolyl side-chain that are commonly referred to as the tau (τ) and pi (π)

positions. Based on known ribosylated and ADP-ribosylated histidine metabolites, it was hypothesized that the τ-nitrogen acts as ADPr acceptor site (Scheme 1, left). Furthermore, it was reasoned that a 1,4-disubstituted triazole could function as nearly perfect isostere for N(τ)-ADPr-His. Thus, **Chapter 2** describes the convergent synthesis of N(τ)-ADPr-histidine isosteres, referred to as N(τ)-ADPr-His*, via a copper(I)-catalyzed azide-alkyne cycloaddition (CuAAC) between azido-ADP-ribosyl analogues and a peptide sequence of choice, carrying a propargyl glycine at the site of modification (Scheme 1, right). Both α- and β-configured azido-ADPr derivatives have been synthesized (**3** and **4** respectively). The latter required participation of the C-2 ester functionality during glycosylation, while the former was obtained stereoselectively using an imidate donor with a non-participating para-methoxybenzyl ether. Two peptide fragments **1** and **2**, originating from histone PARylation factor 1 (HPF1) and poly-ADP-ribose polymerase 1 (PARP1) respectively, were assembled by Fmoc-based solid phase peptide synthesis (SPPS) and successfully conjugated to the azide-modified ADPr. The resulting four N(τ)-ADPr-His* peptides **5α**, **5β**, **6α** and **6β** were screened against a library of human hydrolases known to cleave the glycosidic bond between the distal ribose of ADPr and various amino acid carriers. A slow but consistent hydrolysis of the HPF1 derived isostere **5α** by ARH3 was observed, suggesting a potential role of this enzyme in the reversal of histidine ADP-ribosylation.[3]

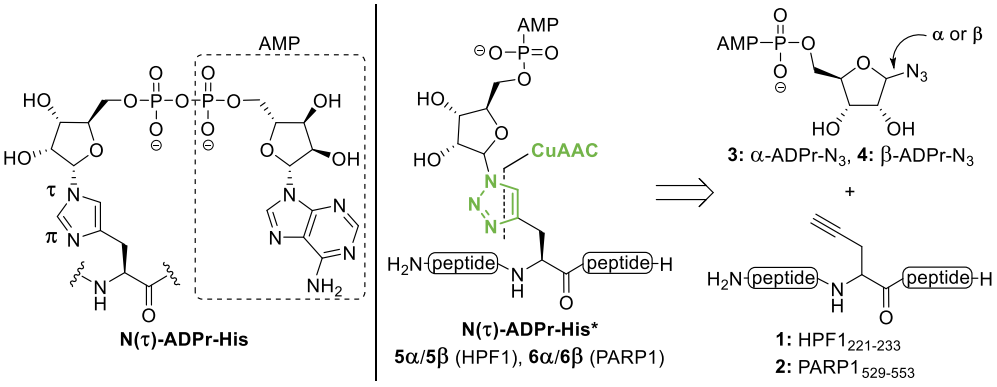

Scheme 1 | The chemical structure of α-N(τ)-ADP-ribosylated histidine (left) and an overview of the work described in Chapter 2, where a late-stage CuAAC is exploited in the synthesis of 1,4-triazolyl linked ADPr-conjugates as isostere for N(τ)-ADPr-histidine (right). The full peptide sequences are $HPF1_{221-233}$ = T-F-H*-G-A-G-L-V-V-P-V-D-K and $PARP1_{529-553}$ = G-G-A-A-V-D-P-D-S-G-L-E-H*-S-A, where the modification site is depicted by H*.

Expansion of the histidine ADP-ribosylation toolbox with 1,5-triazoyl-linked ADPr peptides as isosteres for the N(π)-ADP-ribosylated regioisomer of histidine through the lesser known ruthenium(II)-catalyzed click reaction (RuAAC) is discussed in **Chapter 3**.[4] Since a late-stage functionalization of alkyne-modified oligopeptides with azido-ADP-ribosyl analogues described in Chapter 2 proved incompatible with the RuAAC, an alternative SPPS approach has been

developed that allowed for the synthesis of both 1,4- and 1,5-disubstituted triazole-based histidine isosteres (Scheme 2). Suitably protected propargylglycines **7-8** were conjugated to α- and β-configured ribosyl-azides **9-10** via either a copper(I)- or ruthenium(II)-catalyzed click reaction (Scheme 2). A total of four ribosylated building blocks (**11-14**) were incorporated in a peptide sequence originating from HPF1 using Fmoc-based SPPS, followed by the on-resin installation of the ADP-ribosyl moiety through a P^{III}-P^{V}-coupling method.[5,6] The chemical stability of the resulting ADPr conjugates **5α**, **5β**, **15α** and **15β** was evaluated under various conditions (TFA, NH_2OH and NaOH). No signs of degradation were observed for any of the isosteres using liquid-chromatography mass-spectrometry (LC-MS) under acidic conditions (0.1M TFA) or in the presence of a neutral nucleophile (0.5M, NH_2OH) for at least 24 h. However, the 1,5-disubstituted triazoles **15** were found to be susceptible to a base-assisted (0.1M NaOH) epimerization of the peptide backbone. Finally, their resistance towards (ADP-ribosyl)hydrolase mediated degradation was assessed. In contrast to the inefficient and slow conversion of N(τ)-ADPr-His* **5α** as observed earlier,[3] ARH3 effectively released the modification from the N(π)-ADPr-His* regioisomer **15α**. These findings provided further support for the role of ARH3 in the removal of ADPr from histidine residues.

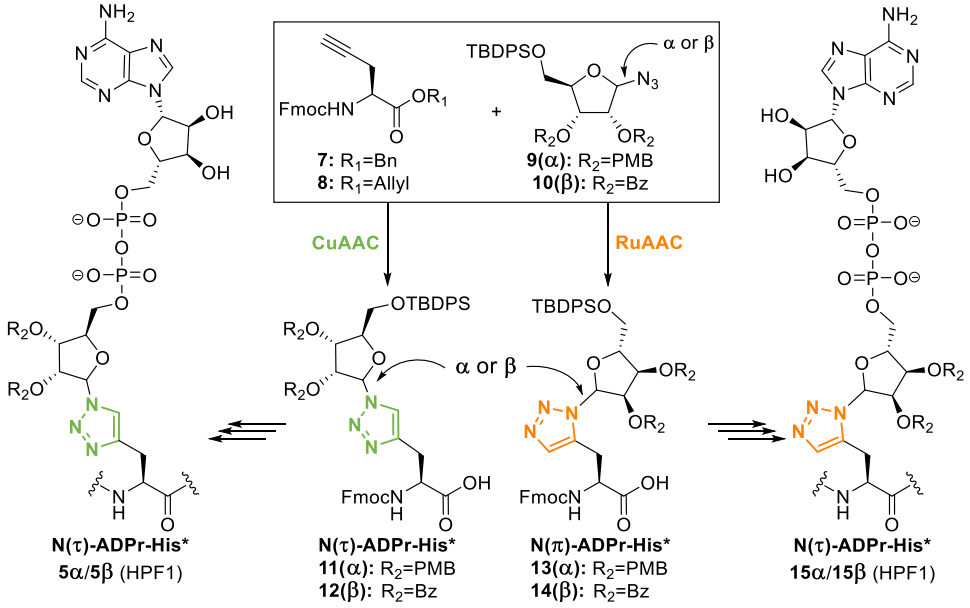

Scheme 2| Overview of the the work described in Chapter 3, where SPPS-compatible ribosylated building blocks were obtained via an early-stage Cu(I)- or Ru(II)-catalyzed click reaction. The full $HPF1_{221-233}$ peptide sequence = T-F-H*-G-A-G-L-V-V-P-V-D-K, where H* refers to the triazole isostere.

With a complete set of triazolyl-linked ADPr conjugates as isosteres for ADP-ribosylated histidine in hand, efforts were made to synthesize peptides with the native ADPr-imidazole linkage. **Chapter 4** describes a synthetic strategy towards N(τ)- and N(π)-ADP-ribosylated histidine

containing peptides **21-22** using a modified Mukaiyama glycosylation reaction[7,8] between ribosyl donor **18** and suitably protected histidine acceptors **16-17**, as a key reaction in the preparation of SPPS-compatible ribosylated histidine Fmoc-building blocks (Scheme 3). Notably, only three distinct mono-ribosylated histidine products could be obtained and, according to HMBC and NOESY measurements, these were assigned as the α-N(π), α-N(τ) and β-N(τ) isomers (**19α**, **20α** and **20β** respectively). A peptide sequence originating from HPF1 was assembled with the ribosylated building blocks using standard Fmoc-based SPPS conditions. In order to finalize the ADPr modification, the immobilized peptides were subjected to the same series reactions as reported for the triazolyl-based isosteres described in Chapter 3. Both the chemical and enzymatic stability of the newly derived peptides **21α**, **22α** and **22β** were evaluated. All three ADPr-His peptides were stable under acidic conditions (0.1M TFA) or in the presence of a nucleophile (0.5M NH_2OH). The behavior of N(π)-regioisomer **21α** under alkaline conditions (0.1M NaOH) was in line with its 1,5-disubstituted triazole counterpart **15α** as base-catalyzed isomerization was observed by LC-MS. Surprisingly, none of the tested human (ADP-ribosyl)hydrolases, including ARH3, were able to hydrolyze the *N*-glycosidic linkage of the three ADP-ribosylated histidine isomers, indicating that the previously observed hydrolytic activity of ARH3 towards **5α** and **15α** is unlikely of any biological relevance. Even though the triazole is arguably the closest imidazole mimic possible, it does differ from its native counterpart and the lower pK_a of the triazole is likely at the basis of the faster hydrolysis by ARH3.

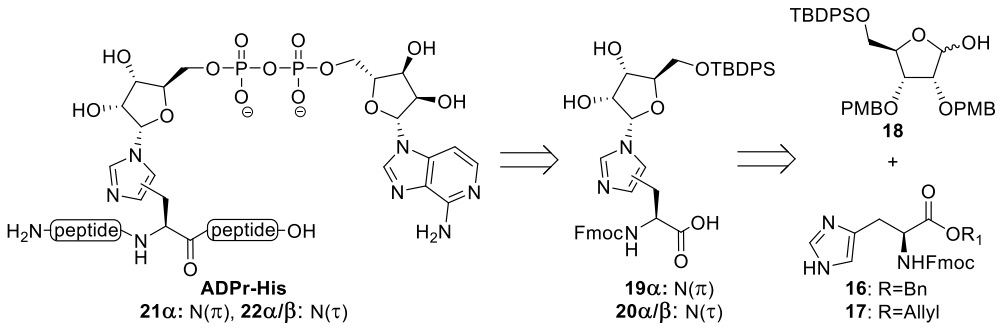

Scheme 3| Retrosynthetic analysis of ADPr-His peptides from Chapter 4, where SPPS-compatible ribosylated histidine building blocks were synthesized via a base-assisted Mukaiyama-like glycosylation procedure.

With respect to the missing β-configured N(π)-ADPr-His isomer, it would be worthwhile to explore different histidine glycosylation methods. To this end, a β-directing ribofuranoside donor with a participating C-2-O-acetyl functionality was subjected to the modified Mukaiyama procedure described in Chapter 4. These attempts failed and ^{31}P NMR analysis of the reaction mixture revealed that the activation of the ribosyl donor with the tributylphosphonium salt did was unsuccessful. An attractive alternative may potentially be found in the gold(I)-catalyzed glycosylation of shelf stable, and readily attainable, *O*-alkynylbenzoate donors.[9,10] This

glycosylation uses only a catalytic amount of the promoter (Au(I) complex), is performed under acid-free conditions and is operationally simple. More importantly, the type of reaction has been applied for the construction of *N*-glycosidic linkages and its stereoselectivity can be steered by participating protecting groups.[11–14]

Ortho-cyclopropylethynyl benzoic acid **25**[15] is more cost-effective than the more frequently used hexynyl analogue[9] and can be derived from its commercially available precursors ethynyl cyclopropane **23** and methyl-2-iodobenzoate **24** via a Sonogashira coupling and subsequent alkaline saponification of the methyl ester functionality (Scheme 4). An EDC-mediated condensation of the carboxylic acid with the anomeric hydroxyl of ribofuranosides **26** and **27** in the presence of DMAP as nucleophilic catalyst could provide the respective benzoate donors **28** and **29**. Glycosylation of allyl protected histidine acceptor **30** with these donors can be achieved under catalysis of $Ph_3PAuNTf_2$[16] and potentially provides N(π)- and N(τ)-ribosylated isomers (**31-32** and **33-34** respectively) with a high level of stereochemical control.

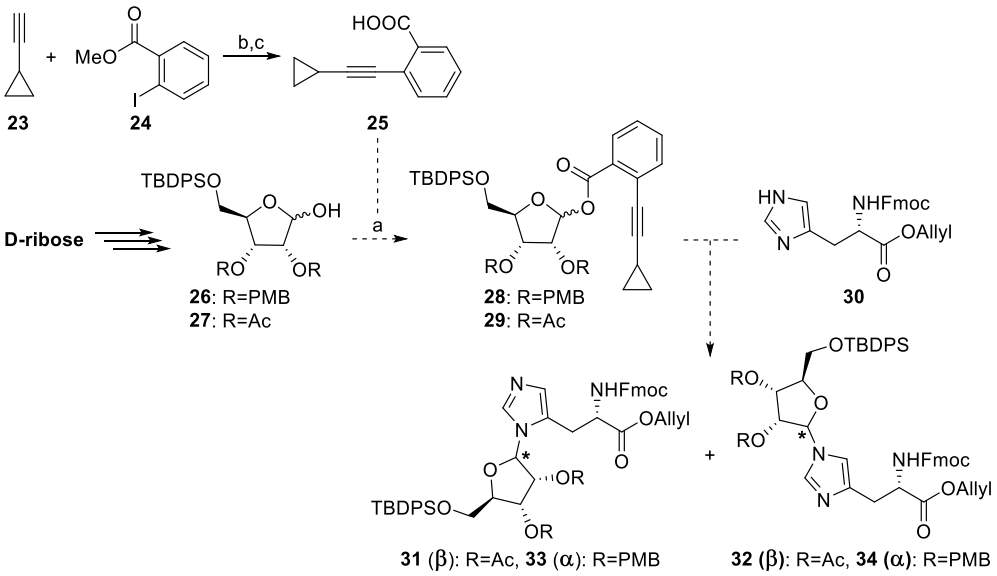

Scheme 4| Proposed gold(I)-catalyzed ribofuranosylation of histidine acceptor **8** as alternative for the Mukaiyama-like glycosylation. Reagents and conditions: a) $Pd(PPh_3)_2Cl_2$, CuI, PPh_3, DIPA, rt. b) NaOH, THF, 50 °C. c) EDC, DMAP, DIPEA, DCM, rt. d) $Ph_3PAuNTf_2$, DCM, rt. DMAP = 4-dimethylaminopyridine and EDC = 1-Ethyl-3-(3-dimethylaminopropyl)carbodiimide.

The unusual amino acid diphthamide is a unique derivative of histidine that is preserved in most eukaryotic lifeforms, but exclusively found on the protein synthesis elongation factor 2 (Scheme 5A).[17,18] Its formation requires an elaborate biosynthetic pathway that includes the transfer of an 3-amino-3-carboxypropyl group from S-adenosylmethionine to the imidazolyl C-2 position followed by per-methylation of the amine functionality and an adenosine

triphosphate (ATP)-driven amidation of the carboxylic acid.[19] Although the biological role of diphthamide remains elusive, its pathological relevance is well-studied.[20] The imidazolyl τ-nitrogen of diphthamide has been identified as one of the first ADP-ribosylation sites that is targeted by an exotoxin secreted by *Corynebacterium diphtheriae*, termed diphtheria toxin (DT), to halt cellular protein synthesis and cause the eponymous disease diphtheria.[21,22] Given that ADP-ribosylated histidine has been successfully prepared, it would be an interesting challenge to develop a methodology for the synthesis of diphthamide containing peptides and the ADP-ribosylated analogues thereof as additional tools to investigate ADP-ribosylation.

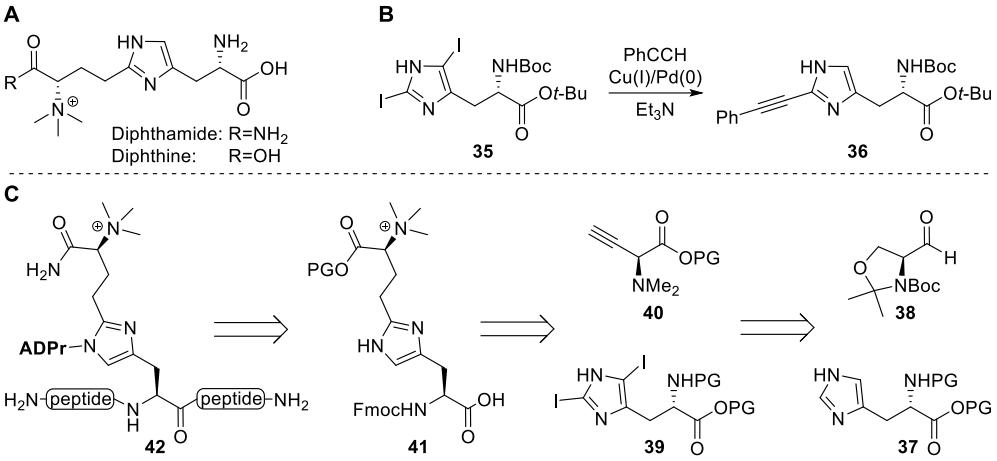

Scheme 5| A. chemical structure of diphthamide (R=NH_2) and its carboxylic acid precursor diphthine (R=OH). B. The cross-coupling between diiodo hisitidine analogue **35** and phenylacetylene as reported by Evan *et al.*[24] C. A projected chemoenzymatic approach towards oligopeptides ADP-ribosylated on diphthamide, a unique C-2 functionalized analogue of histidine present in the sequence of elongation factor 2.

Literature precedent regarding the synthesis of diphthamide, or its carboxylic acid precursor diphthine, is rather limited with two distinct synthetic routes reported by the laboratory of Evans.[23,24] In one of these papers a simultaneous C-5 dehalogenation and cross-coupling on the more electron deficient imidazolyl C-2 position was described for a 2,5-diiodohistidine analogue **35** with phenylacetylene (Scheme 5B), which forms the foundation for the route towards peptides ADP-ribosylated on diphthamide **42**, as proposed here (Scheme 5C).[24] It is envisioned that a peptide sequence of choice can be assembled with diphthine building block **41** using Fmoc-based SPPS chemistry, followed by amidation of the ester functionality with trifluoroethanol and ammonia. DT-mediated ADP-ribosylation can then provide the fully functionlized ADPr-diphthamide peptides.[25] The required building block can potentially be obtained through the above mentioned tandem dehalogenation/cross-coupling reaction using suitably protected ethynylglycine **40** and 2,5-diiodohistidine **39**. The synthetic endeavor

towards these precursors can be initiated from Garner's aldehyde **38**[26,27] and protected histidine **37** respectively.

Initial exploratory work on the iodination of histidine and the regioselective C-2 functionalization with model alkynes has been performed as shown in Scheme 6. Fully protected histidine **43** was first detritylated with trifluoroacetic acid (TFA) in the presence of triisopropylsilane (TIS) as cation scavenger followed by an overnight electrophilic aromatic substitution (EAS) with *N*-iodisuccinimide (NIS) in acetonitrile to provide 2,5-iodinated histidine **44**.[28] Unfortunately, the Fmoc-protecting group was cleaved during the modified Sonogashira cross-coupling procedure with phenylacetylene as model substrate and prevented product formation.[24] Instead, a series of protecting group manipulations provided benzyloxycarbonyl (Cbz)-protected analogue **47**, which was iodinated uneventfully using identical conditions as its Fmoc-counterpart to provide 2,5-diiodohistidine **48**. In accordance with the observations reported by Evans, C-2 functionalized histidine **49** was obtained in a satisfactory yield during the initial test reaction with phenylacetylene. Minor changes in reaction conditions also allowed regioselective functionalization of iodinated precursor **48** with 1-hexyne to yield aliphatic alkyne **50**. Future attempts will have to demonstrate if histidine can be coupled to more complex alkynes such as ethynylglycine derivatives via this procedure.

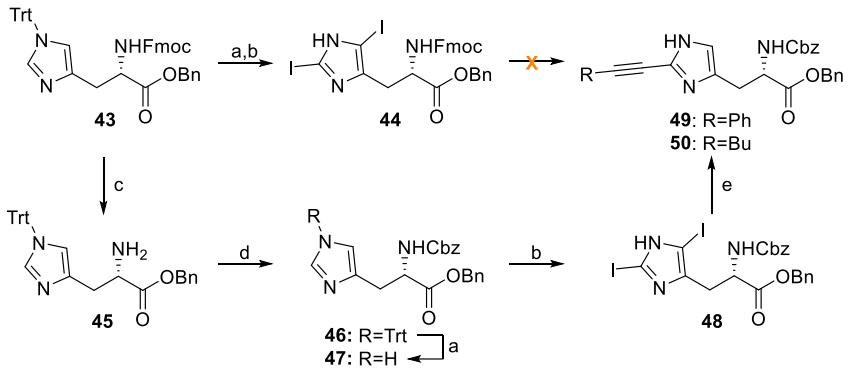

Scheme 6| Synthesis of diiodo-histidine analogues **44** and **48** followed by a regioselective functionalization with model alkynes. Reagents and conditions: a) TFA, TIS, DCM, rt, 4 h (100% for **47**). b) NIS, MeCN, dark, rt, 16 h (59% for **44**, 72% for **48**). c) Piperidine, DCM, rt , 30 min (78%). d) Cbz-OSu, Et_3N, MeCN, rt, 1 h (100%), e) phenylacetylene or hex-1-yne, $(PPh_3)_2PdCl_2$, CuI, Et_3N, THF or DMF, 65 °C, 16 h (42% for **49**, 34% for **50**).

Carba-sugars that are equipped with an electrophilic warhead, like the epoxide containing natural product cyclophellitol,[29] have been demonstrated to function as covalent and irreversible mechanism-based inhibitors for glycosidases by 'trapping' the catalytic nucleophile in the active site. The collection of electrophilic traps include epoxides,[30] (substituted) aziridines,[30] and as of recently, cyclic sulfates.[31] While pyranose-based inhibitors have been

extensively studied, furanose-derived inhibitors equipped with electrophilic functionalities, have attracted less attention, with the notable exception of the work on arabinofuranosidase inhibitors.[32,33] Therefore, **Chapter 5** describes an exploratory study on the synthesis and evaluation of carba-ribofuranoside-based sulfates **51** and 2-deoxy analogue **52** as potential glycosidase inhibitors (Figure 1). The synthetic endeavor was initiated from D-mannose and included a ring-closing metathesis, a [2+3]-Wittig-Still rearrangement, a stereoselective *cis*-dihydroxylation, and a radical-mediated Barton McCombie deoxygenation as key reactions. The exact stereochemistry of the cyclic sulfate functionalities has been determined with the help of NOESY measurements. Preliminary testing of the newly delivered warheads in a 4-methylumbelliferone (4-MU)-based fluorogenic assay with readily available glucosidases and mannosidases revealed a high millimolar inhibition of acid α-glycosidase (GAA) by cyclosulfate **51α**. A more elaborate screening may disclose the inhibitory potential of the cyclosulfate warheads on other glycosidases.

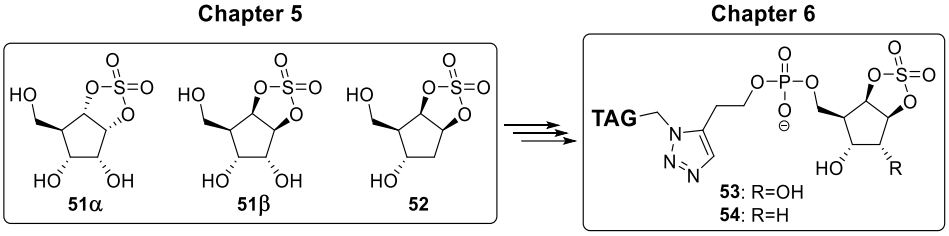

Figure 1| Chemical structures of the cyclosulfate warheads that were synthesized and evaluated as potential glycosidase inhibitors (Chapter 5). Incorporation of the β-configured cyclosulfates into potential activity-based probes for CD38 with a sulforhodamine-based fluorescent reporter as 'TAG' (Chapter 6).

Transmembrane protein cluster of differentiation 38 (CD38) is located on the surface of immune cells where it not only functions as receptor,[34] but also catalyzes an impressive collection of chemical conversions of its substrates NAD^+ and 2'-phosphorylated analogue $NADP^+$.[35,36] Crystallographic studies have revealed that the CD38 can be inhibited, in a substrate-dependent manner, through the formation of a stable covalent inhibitor-enzyme intermediate in which the inhibitor was bound to the catalytic glutamate residue, in line with the covalent inhibition of glycosidases.[37,38] Structural activity relationship studies with various NAD^+ and nicotinamide mononucleotide (NMN^+) analogues indicated that adenosine monophosphate (AMP) is not crucial for inhibition,[39,40] which eventually led to the development of activity-based probe (ABP) SR101-F-araNMN$^+$ **55** by Liu *et al* (Figure 2A).[41] Inspired by these findings, the use of β-configured cyclosulfates **51β** and **52** in potential mechanism-based ABPs for CD38 was explored and the corresponding synthesis is described in **Chapter 6** (Figure 1). Regioselective phosphorylation of the primary alcohol of the cyclosulfates was achieved through a dicyanoimidazole (DCI)-mediated phosphoramidite coupling, which required an acid-labile protecting group strategy due to lability of the cyclic sulfate moiety under basic conditions. An alkyne click handle on the newly introduced phosphate group allowed for a Cu(I)-mediated

conjugation to an azide-modified sulforhodamine 101 reporter tag and provided ABPs **53** along with its 2-deoxy analogue **54**.

The inhibitor potential of both compounds against CD38 remains to be evaluated. HL-60 cells provide a convenient model system as CD38 is completely absent under regular conditions, but can be upregulated by all-trans retinoic acid (RA)[42] via a RA receptor-α mediated pathway.[43] Hence, RA-induced HL-60 cells can be used as positive control, while untreated cells are suitable negative controls in labeling studies. A sample of the validated ABP **55** was kindly donated by the laboratory of Liu[41] and used for the optimization of the assay conditions (Figure 2B). HL-60 cells were incubated with RA or DMSO for 48 h, collected and subsequently incubated with various concentrations of SR101-F-araNMN$^+$ **55**. Initially, cell lysis was attempted by repeatedly pushing the lysate through a 25 gauge injection needle. However, this method was too mild by itself and did not provide the desired membrane protein pellets after centrifugation unless the cells had been stored at -80 °C prior. After separation of the membrane proteins using gel electrophoresis, a clear fluorescent signal (Cy3 channel) was exclusively obtained in the RA-samples at the approximate height expected for CD38 (45kDa, Figure 1C). In a follow-up experiment, it was determined that a 2 µM inhibitor concentration was optimal under the given conditions. Finally, the proteins have been transferred to a western blot membrane and treated overnight with different dilutions (500x versus 250x) of an anti-CD38 antibody obtained from BD Transduction Laboratories™ (#61114) to confirm the identity of the labeled protein. A clear chemiluminescent signal was observed for the 500x antibody dilution, which corresponded with the fluorescent band observed earlier on SDS-PAGE. Through these experiments, the RA-induced expression of CD38 by HL-60 cells has been validated, opening the way to the future evaluation of cyclosulfate **53** and **54** as potential ABPs for CD38.

It is conceivable that α-configured cyclosulfate **51α** can be used in the development of substrate-based covalent inhibitors for (ADP-ribosyl)hydrolases and their corresponding ABPs. For example, phosphotriester **57** has been derived from its precursor using the identical two-step procedure as described in Chapter 6, where the regioselective introduction of *t*-butyl protected phosphoramidite **56** is immediately followed by oxidation of the P^{III}-intermediate with *t*-BuOOH (Scheme 7). Deprotection of the phosphate with HCl in HFIP,[44] efficiently provided carba-ribosyl cyclosulfate **58** in high purity after a simple washing procedure. The alkyne functionality allows for a straightforward functionalization of the potential inhibitor with various azide-modified reporter tags, such as SR101-N_3, through a CuAAC to provide ABPs of general structure **59**.

In addition, a synthetic route towards carba-ADPr counterpart **67** is proposed based on the report of a simple one-pot reaction for the production of sugar nucleoside diphosphates.[45] First, the activating reagent 2-imidazolyl-1,3-dimethylimidazolinium chloride (ImIm) is made *in situ* from 2-chloro-1,3-dimethyl-imidazolinium chloride (DMC) and imidazole (Scheme 7). Then, a reactive phophorimidazolidate is formed by adding the unprotected nucleotide to enable a

P^V-P^V coupling with the phosphorylated saccharide. To this end, alkyne-modified adenosine **63** can be prepared through amination of inosine with propargylamine.[46,47]

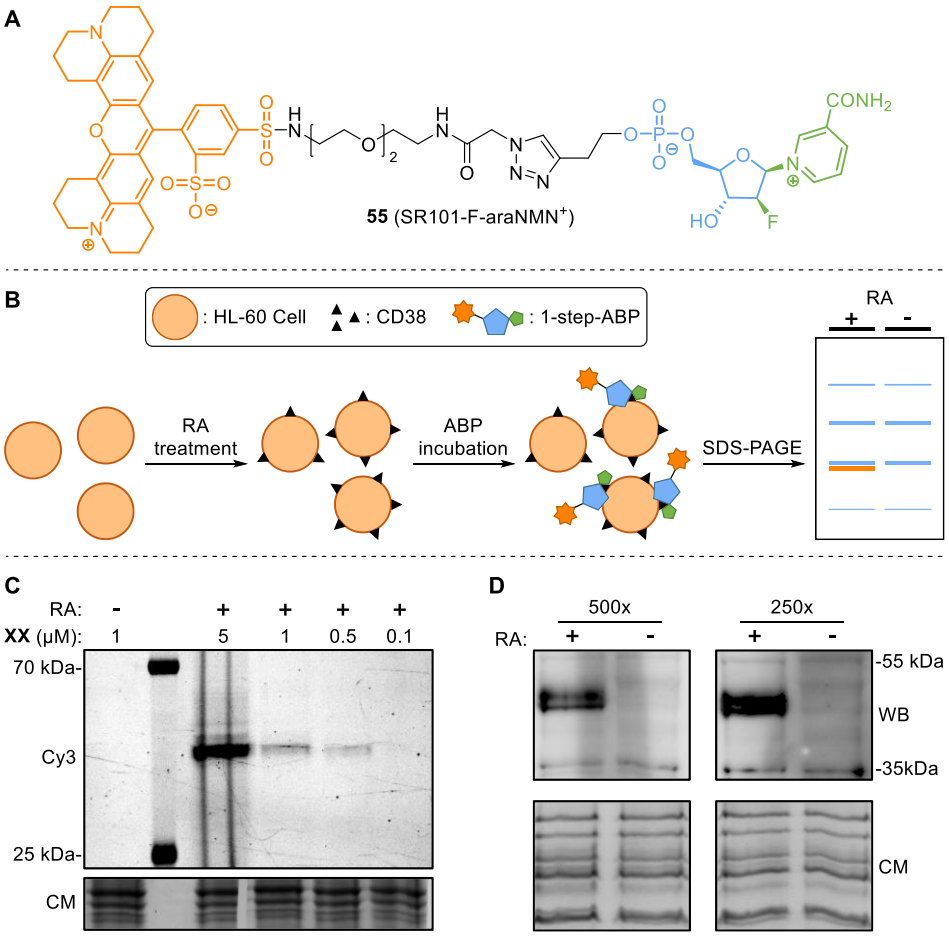

Figure 2| A. Chemical structure of the validated 1-step ABP **55** as reported by Liu *et al.*[41] B. Schematic overview of a biochemical assay with HL-60 cells that can be applied for the evaluation of new 1-step ABPs. C. In-gel fluorescence analysis of HL-60 membrane protein fractions incubated with different concentrations of ABP **55**. D. Western blot analysis of the membrane protein fractions with various dilutions of the anti-CD38 antibody (500x and 250x respectively). Coomassie staining is included as protein loading control. Cy3 = cyanine dye 3 (565 nm), WB = western blot, CM = Coomassie stain and RA = all-trans retinoic acid.

A change to bis(*tert*-butyl)-protected amidite **60** in the two-step phosphorylation method followed by HCl-mediated deprotection of the acid-labile protecting groups could provide free phosphomonoesters **62** and **65** from their respective precursors **51a** and **63**. The pyrophosphate linkage in cyclosulfate-based carba-ADPr analogue **66** can then potentially be

constructed via the above mentioned imidazolidate chemistry. Ultimately, the synthetic endeavor towards **67** is completed with a Cu(I)-mediated conjugation to the sulforhodamine reporter tag.

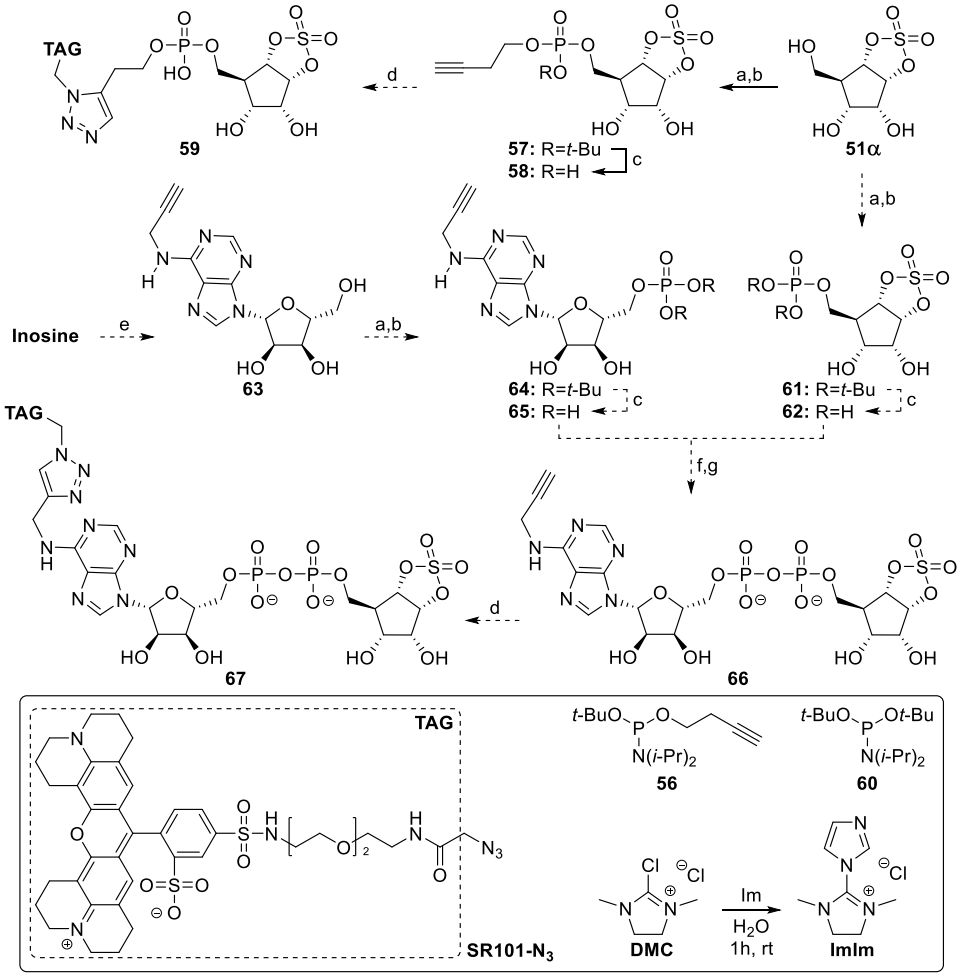

Scheme 7| Proposed synthetic route towards cyclosulfate-based NMN^+ and NAD^+ analogues as potential activity-based probes for ARHs. Reagents and conditions: a) **56** or **60**, DCI, MeCN, 0 °C, 1h. b) *t*-BuOOH, MeCN, 0 °C, 1.5 h (36% over 2 steps for **57**). c) HCl, TIS, HFIP, rt, 1.5 h (59% for **58**). d) SR101-N_3, $CuSO_4$, sodium ascorbate, THPTA, DMF, rt, 1 h. e) propargylamine, BOP, DIPEA, DMF 24 h. f) Imidazole, DMC, **65**, D_2O, rt, 1 h. g) **62**, rt, 16 h.

Experimental

General biological procedures

All-trans Retinoic acid (RA) was purchased from Focus Biomolecules (Cat# 10-1138) and dissolved in DMSO (molecular biology grade, D8418) to provide a 1 mM stock solution. 25 gauge BD microlance™ 3 injection needles (0.5x25mm, orange) were used in the preparation of cell lysates. A stock solution of the validated CD38 inhibitor SR101-F-araNMN (0.49 mM in DMSO) was obtained from the group of Hening Lin at the department of chemistry & chemical biology of the Cornell University.[41] Lysis buffer recipe: sucrose (250 mM), Tris-HCl (pH=7.9, 50 mM) and $MgCl_2$ (5 mM) and freshly supplemented with protease inhibitor cocktail (PIC, 1x) and dithiothreitol (DTT, 1 mM). PageRuler™ Plus (10 to 250 kDa, Thermo Fisher) was used as protein marker for sodium dodecyl sulfate–polyacrylamide gel electrophoresis (SDS-PAGE). Fluorescence and chemiluminescence were measured using a Bio-Rad ChemiDoc MP imaging system and analyzed using the Image Lab 6.0.1 software. Proteins were transferred onto a mini-format polyvinylidene difluoride (PVDF, 0.2 µm) membrane (Bio-Rad, #1704156) using the Bio-Rad Trans-Blot Turbo Transfer System. The Clarity™ Western ECL peroxide and luminol reagents (Bio-Rad, #1705060S) were used to develop western blot membranes and provide chemiluminescence signals. The purified mouse anti-human CD38 antibody was obtained from BD Transduction Laboratories™ (#61114, 50 µg) and was used in combination with the goat anti-mouse antibody conjugated to horseradish peroxidase (HRP) from Santa Cruz Biotechnology (Cruz Marker, SC-516102-CM).

Cell passaging of HL-60 cells

HL-60 cells were cultured at 37 °C under 7% CO_2 in RPMI-1640 medium buffered with 25 mM HEPES (Sigma Aldrich R5886) containing phenol red pH indicator and freshly supplemented with L-alanine-L-glutamine (Glutamax, a stable glutamine precursor), 10 v/v% Newborn Calf Serum (NBCS, Thermo Fisher) and 200 µg/ml penicillin and streptomycin (Duchefa). Cell viability and concentration was determined twice a week by diluting a cell suspension sample (10 µl) with 0.4 w/v% Trypan blue solution (10 µl), which was subsequently analyzed with a Bio-Rad TC20 automated cell counter. Cells were passaged accordingly by dilution with fresh medium to a final concentration of 2-2.5x10^5 cells/ml. Cultures were discarded after 2-3 months of passaging.

HL-60 Cell pellet preparation

5x10^6 cells were re-suspended in fresh medium and added to a Sarstedt petri dish (⌀ = 10 cm). The cells were incubated for 48-72 h with either retinoic acid (1 µM final concentration) or DMSO (control). Afterwards, cells were harvested by pipetting and centrifuged (25 °C, 200 rcf, 5 min), followed by removal of the medium. The pellets were re-suspended in phosphate buffer saline (PBS, 1 ml), centrifuged (25 °C, 200 rcf, 5 min) followed by removal of the supernatant. These washing steps were repeated once more before the pellets were frozen in liquid nitrogen and stored at -80 °C until further use.

SDS-PAGE analysis of HL-60 membrane proteins

Cell pellets (48 h stimulation with RA or DMSO) were thawed on ice, re-suspended in lysis buffer (350 µl) and incubated for 30 min at 0 °C before carefully pushing the suspension through an injection needle (10x). The suspension was centrifuged (4 °C, 15 min, 800 rcf) and the majority of the supernatant (250 µl) was collected. SR101-F-araNMN (0.2 µl of 0.49 mM stock) was added to a portion of the resulting supernatant (50 µl) to provide a 2 µM concentration. After incubating for 15 min at rt, the samples are centrifuged (4 °C, 28.000 rcf, 60 min) and the supernatant containing cytosolic proteins is removed. The membrane pellets are re-suspended in 2x Laemmi buffer (30 µl), heated to 95 °C for 5 min and subsequently loaded (20 µl per well) on a 10% SDS-PAGE gel along with protein marker (3 µl). An voltage (15 min at 80 V, 120

min at 120 V) was applied and fluorescence was measured for 60 seconds in the Cy3- and Cy5-channel. Afterwards, the gel was stained with Coomassie and imaged as a loading control for normalization.

Western blot analysis of HL-60 membrane proteins

Cell pellets (72 h stimulation with RA or DMSO) were thawed on ice, re-suspended in lysis buffer (200 µl) and incubated for 30 min at 0 °C before carefully pushing the suspension through an injection needle (10x). The suspension was centrifuged (4 °C, 800 rcf, 15 min) and the supernatant was collected and centrifuged again (4 °C, 28.000 rcf, 60 min). After removal of the supernatant containing cytosolic proteins, the membrane pellet was dissolved in 2x Laemmi buffer (100 µl), heated to 95 °C for 5 min and subsequently loaded (15 µl per well) on a 12.5% SDS-PAGE gel along with protein marker (3 µl). A voltage (80 min at 200 V) was applied and the proteins were subsequently transferred to a PVDF membrane (7 min, 1.3 A, 25 V). The membrane was washed with milliQ water (15 ml) and Tris-Buffered Saline (TBS, 15 ml) before blocking with 5% w/v non-fat dry milk in TBS-Tween© buffer (TBST, 10 ml) for 1 h at rt. The membrane was washed with TBST (3x 15 ml) and blocked for an additional 15 min with 5 w/v% BSA in TBST (10 ml). Anti-human CD38 antibody (40 µl → 1:250 dilution) was added to the TBST solution and the membrane was incubated overnight at 4 °C. The blot was washed with TBST (3x 10 ml for 5 min), TBS (3x 10 ml for 5 min) and blocked with 5% w/v bovine serum albumin (BSA) in TBST (10 ml) for 15 min. The secondary anti-mouse antibody (4 µl → 1:2500 dilution) was added and shaken for 1 h at rt. After washing with TBST (3x 10 ml for 5 min), TBS (3x 10 ml for 5 min) and finally milliQ water (3x 10 ml for 5 min), the membrane was treated with H_2O_2 and luminol in the absence of light for several minutes. Chemiluminescence was detected in the corresponding channel and the protein marker was visualized using the colorimetric channel. Images were processed using Image lab 6.0.1.

General synthetic procedures

All chemicals were used as received unless stated otherwise. 2-azidoacetic acid was derived from bromoacetic acid according to a reported literature procedure.[48] $SnCl_4$ (1 M in DCM) and *t*-BuOOH (5.5 M in nonane) were purchased at Sigma Aldrich. Dowex 50WX8 hydrogen form (100-200 mesh) was purchased at Sigma Aldrich and washed with H_2SO_4 (5 M, 3x) and MeOH (3x) prior to use. Molecular sieves were flamedried (3x) in vacuo before use. Solvents were dried over activated 4Å molsieves for 24 h except for MeCN and MeOH which were dried over 3Å molsieves. A solution of HCl (0.2 M in HFIP) was freshly prepared prior to the reaction by dissolving HCl (37%, 0.1 ml) to HFIP (5.9 ml). Silica 60 M (0.04-0.063 mm) from Macherey-Nagel GmbH was used in combination with solvents of technical grade from Sigma Aldrich for silica gel column chromatography. High-purity grade silica gel (Davisil 633, #236772) used in the purification of the described phosphoramidites was purchased from Sigma Aldrich. After use the silica was washed with MeOH and Et_2O and thoroughly dried in an oven (80 °C) for several hours prior to its next use. Reactions were performed under N_2 atmosphere unless stated otherwise. A FutureChemistry NE 1000G syringe pump was used for slow and constant addition of reagents when stated. Reaction mixtures were concentrated under reduced pressure using rotary evaporators at 40-45 °C unless state otherwise. Reactions were monitored by thin layer chromatography (TLC) analysis using silica gel 60 F254 coated aluminum sheets from Merck. TLC plates were visualized with ultraviolet light (254 nm) or sprayed with H_2SO_4 (20% v/v in MeOH), potassium permanganate (1 g $KMnO_4$, 5 g K_2CO_3, in 200 ml H_2O) or ceric ammonium molybdate (1 g $Ce(NH_4)_4(SO_4)_4 \bullet 2H_2O$, 2.5 g $(NH_4)_6Mo_7O_{24} \bullet 4H_2O$, 10 ml H_2SO_4 in 90 ml H_2O). Infrared (IR) values are reported in cm^{-1}. ^1H NMR, ^{13}C NMR and ^{31}P NMR spectra were recorded on Bruker AV-300 (300 mHz), AV-400 (400 mHz) or AV-500 (500 mHz) spectrometer. ^{13}C NMR spectra are acquired via the attached proton test (APT) experiment and are presented with even signals (C_q and CH_2) pointing upwards and odd signals (CH and CH_3) pointing downwards. The chemical shifts are noted as δ-values in parts per million (ppm) relative to the tetramethylsilane signal (δ = 0 ppm) or solvent signal of D_2O (δ =

4.79 ppm) for ^{1}H NMR and relative to the solvent signal of $CDCl_3$ (δ = 77.16 ppm) for ^{13}C NMR. Phosphorylation reactions were monitored with ^{31}P NMR using an acetone-D_6 insert for a locking signal and the resulting spectra were indirectly calibrated with H_3PO_4. HRMS samples were prepared in either MeOH, MeCN or milliQ grade H_2O with an approximate concentration of 1 mM and measured on a Thermo Scientific LTQ Orbitrap XL.

2,5-diiodo-N_α-Fmoc-L-histidine benzyl ester (44).

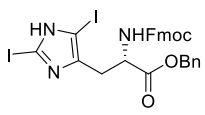

A solution of **43** (0.61 mmol, 0.29 g) in MeCN (4 ml) was purged with argon before adding *N*-iodosuccinimide (1.5 mmol, 0.34 g) and the resulting suspension was stirred overnight in the dark at rt. The reaction mixture was concentrated under reduced pressure followed by the addition of EtOAc (9 ml) and $Na_2S_2O_3$ (sat., 0.9 ml). After 15 min, the organic layer was washed with brine (2x 20 ml), dried over $MgSO_4$, and concentrated under reduced pressure. Purification of the crude residue by silica gel column chromatography (pentane/EtOAc = 60:40) yielded title compound **44** (0.36 mmol, 0.26 g, 59%) as a yellow solid. $\mathbf{R_f}$ = 0.76 (pentane/EtOAc = 20:80). **^{1}H NMR** (500 MHz, $CDCl_3$): δ 7.68 (d, *J* = 7.6 Hz, 2H), 7.49 (d, *J* = 7.9 Hz, 2H), 7.37 – 7.16 (m, 9H), 6.17 – 5.84 (m, 1H), 5.09 (q, *J* = 12.2 Hz, 2H), 4.69 – 4.51 (m, 1H), 4.36 – 4.27 (m, 2H), 4.15 – 4.05 (m, 1H), 3.16 – 2.95 (m, 2H). **^{13}C NMR** (126 MHz, $CDCl_3$): δ 171.0, 156.2, 143.6, 143.5, 141.3, 141.2, 134.8, 128.7, 128.6, 128.4, 127.8, 127.2, 127.2, 125.2, 120.0, 67.8, 67.5, 53.7, 47.0, 29.4. **HRMS** $[C_{28}H_{23}I_2N_3O_4 + H]^+$ = 719.9838 found; 719.98507 calculated.

$N_{(im,\tau)}$-trityl-L-histidine benzyl ester (45).

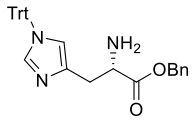

A solution of **43** (5.5 mmol, 3.9 g) and piperidine (91 mmol, 9 ml) in DCM (36 ml) was stirred for 30 min at rt. The reaction mixture was washed with $NaHCO_3$ (3x 30 ml) and the organic layer was dried over $MgSO_4$, and concentrated under reduced pressure. Purification of the crude residue by silica gel column chromatography (DCM/MeOH = 100:0 → 90:10 + 1% Et_3N) yielded title compound **45** (4.3 mmol, 2.1 g, 78%) as a yellowish liquid. $\mathbf{R_f}$ = 0.2 (DCM/MeOH = 95:5). **^{1}H NMR** (400 MHz, $CDCl_3$): δ 7.38 (s, 1H), 7.36 – 7.23 (m, 14H), 7.15 – 7.05 (m, 6H), 6.57 (s, 1H), 5.06 (q, 2H), 3.85 (dt, J = 7.0, 4.7 Hz, 1H), 2.96 (qd, 2H), 2.06 – 1.77 (m, 2H). **^{13}C NMR** (101 MHz, $CDCl_3$): δ 174.8, 142.2, 138.5, 137.0, 135.6, 129.6, 128.3, 128.0, 128.0, 127.9, 127.8, 119.4, 75.0, 66.3, 54.6, 33.2. **HRMS** $[C_{32}H_{29}N_3O_2 + H]^+$ = 488.23272 found; 488.23325 calculated.

N_α-(benzyloxy)carbonyl-$N_{(im,\tau)}$-trityl-L-histidine benzyl ester (46).

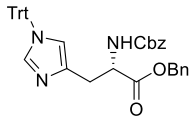

A solution of **45** (0.21 mmol, 0.10 g) in anhydrous MeCN (1.5 ml) was cooled to 0 ^{0}C before adding Et_3N (0.62 mmol, 86 µl) and *N*-(Benzyloxycarbonyloxy) succinimide (0.31 mmol, 77 mg). After 30 min, the reaction mixture slowly warmed to rt and stirred for an additional 30 min before concentrating under reduced pressure. The crude residue was diluted with EtOAc (25 ml), washed with water (3x 25 ml). The organic layer was dried over $MgSO_4$ and concentrated under reduced pressure. Purification of the crude residue by silica gel column chromatography (pentane/Et_2O = 60:40 → 50:50) yielded title compound **46** (0.21 mmol, 0.13 g, 100%) as a clear oil. $\mathbf{R_f}$ = 0.4 (pentane/Et_2O = 30:70). **^{1}H NMR** (400 MHz, $CDCl_3$): δ 7.38 – 7.27 (m, 14H), 7.26 – 7.16 (m, 6H), 7.10 – 7.04 (m, 6H), 6.49 – 6.42 (m, 2H), 5.16 – 4.96 (m, 4H), 4.64 (dt, J = 8.3, 4.8 Hz, 1H), 3.04 (qd, J = 14.6, 4.9 Hz, 2H). **^{13}C NMR** (101 MHz, $CDCl_3$): δ 171.5, 156.2, 142.3, 138.9, 136.6, 136.3, 135.5, 129.8, 128.5, 128.5, 128.3, 128.1, 128.1, 128.0, 119.7, 75.3, 66.9, 66.8, 54.3, 29.8. **HRMS** $[C_{40}H_{35}N_3O_4 + H]^+$ = 622.26963 found; 622.27003 calculated.

N_α-(benzyloxy)carbonyl-L-histidine benzyl ester (47).

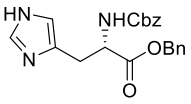

To a solution of **46** (1.2 mmol, 0.72 g) in DCM (11.5 ml) were added TFA (12 mmol, 0.88 ml) and TIS (1.3 mmol, 0.26 ml, 1.1 eq). The reaction mixture was stirred for 4 h at rt before concentrating under reduced pressure. Purification of the crude residue by silica gel column chromatography (DCM/MeOH = 98:2 → 80:20) yielded title compound **47** (1.2 mmol, 0.44 g, 100%) as a clear oil. $\mathbf{R_f}$ = 0.5 (DCM/MeOH = 93:7). **^{1}H NMR** (500 MHz, $CDCl_3$): δ 8.17 (s, 1H), 7.39 – 7.11 (m, 10H), 6.83 (s, 1H), 6.47 (d, J = 8.2 Hz, 1H), 5.09 (q, 2H), 4.96 (q, 2H), 4.66 – 4.58 (m, 1H), 3.16 (td, 2H). **^{13}C NMR** (126 MHz, $CDCl_3$): δ 170.6, 156.3, 136.0, 134.9, 129.2, 128.8, 128.7, 128.7, 128.6, 128.5, 128.5, 128.3, 128.2, 128.0, 117.0, 67.8, 67.2, 53.6, 27.3. **HRMS** $[C_{21}H_{21}N_3O_4 + H]^+$ = 380.15992 found; 380.16048 calculated.

2,5-diiodo-N_α-(benzyloxy)carbonyl-L-histidine benzyl ester (48).

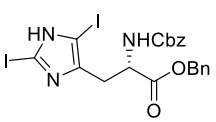

A solution of **47** (1.2 mmol, 0.44 g) in MeCN (7.5 mL) was purged with argon before adding N-iodosuccinimide (2.9 mmol, 0.65 g) and the resulting suspension was stirred overnight in the dark at rt. The reaction mixture was concentrated under reduced pressure followed by the addition of EtOAc (16 mL) and $Na_2S_2O_3$ (sat., 1.6 mL). The organic layer was washed with brine (2x 15 ml), dried over $MgSO_4$ and concentrated under reduced pressure. Purification of the crude residue by silica gel column chromatography (pentane/EtOAc = 70:30 → 60:40) yielded title compound **48** (0.83 mmol, 0.52 g, 72%) as a yellow foam. $\mathbf{R_f}$ = 0.6 (pentane/EtOAc, 50:50). **^{1}H NMR** (400 MHz, $CDCl_3$): δ 10.88 (s, 1H), 7.37 – 7.24 (m, 10H), 6.25 – 5.65 (m, 1H), 5.20 – 5.02 (m, 4H), 4.81 – 4.50 (m, 1H), 3.09 (dd, 2H). **^{13}C NMR** (101 MHz, $CDCl_3$): δ 170.9, 156.2, 135.7, 134.7, 134.0, 128.9, 128.7, 128.6, 128.2, 128.2, 85.1, 83.3, 68.1, 67.7, 60.6, 53.5, 29.6, 14.3. **HRMS** $[C_{21}H_{19}I_2N_3O_4 + H]^+$ = 631.95292 found; 631.95377 calculated.

2-phenylethynyl-N_α-(benzyloxy)carbonyl-L-histidine benzyl ester (49).

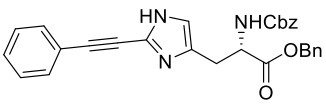

A solution of **48** (0.16 mmol, 0.10 g) in distilled Et_3N (2.2 mL) and anhydrous THF (1 mL) was purged with argon for 10 min before bis(triphenylphosphine)palladium(II) dichloride (16 µmol, 11 mg), CuI (8 µmol, 2 mg) and phenylacetylene (0.48 mmol, 53 µL) were added. The reaction mixture was stirred overnight at 65 °C and concentrated under a flow of nitrogen. Purification of the crude residue by silica gel column chromatography (pentane/EtOAc = 90:10 → 40:60) yielded title compound **49** (70 µmol, 32 mg, 42%) as an orange oil. $\mathbf{R_f}$ = 0.5 (pentane/EtOAc, 50:50). **^{1}H NMR** (400 MHz, $CDCl_3$): δ 10.29 (s, 1H), 7.45 (t, J = 6.2, 1.9 Hz, 2H), 7.37 – 7.19 (m, 13H), 6.66 – 6.50 (m, 1H), 6.25 – 6.09 (m, 1H), 5.14 – 5.06 (m, 4H), 4.76 – 4.63 (m, 1H), 3.27 – 2.89 (m, 2H). **^{13}C NMR** (126 MHz, $CDCl_3$): δ 171.5, 156.3, 131.8, 129.1, 128.6, 128.5, 128.5, 128.4, 128.1, 121.7, 115.0, 90.1, 79.5, 67.0, 54.1, 32.0, 30.3, 29.8, 29.4, 22.8, 14.2. **HRMS** $[C_{29}H_{15}N_3O_4 + H]^+$ = 480.19129 found; 480.19178 calculated.

2-hex-1-yn-1-yl-N_α-(benzyloxy)carbonyl-L-histidine benzyl ester (50).

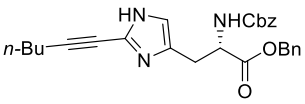

A solution of **48** (0.16 mmol, 0.10 g) in distilled Et_3N (2.2 mL) and anhydrous DMF (1 mL) was purged with argon, before bis(triphenylphosphine)palladium(II) dichloride (16 µmol, 11 mg), CuI (8 µmol, 2 mg) and 1-hexyne (0.48 mmol, 55 µL) were added. The reaction mixture was stirred overnight at 65 °C and concentrated under a flow of nitrogen followed by rotary evaporation. Purification of the crude residue by silica gel column chromatography (pentane/EtOAc = 90:10 → 40:60) yielded title compound **50** (50 µmol, 25 mg, 34%) as an orange oil. $\mathbf{R_f}$ = 0.6 (pentane/EtOAc = 50:50). **^{1}H NMR** (300 MHz, DMSO): δ 7.44 – 7.13 (m, 11H), 6.76 (s, 1H), 5.19 – 4.97

(m, 4H), 4.51 – 4.35 (m, 1H), 3.03 – 2.91 (m, 2H), 2.43 (t, J = 6.9 Hz, 2H), 1.64 – 1.37 (m, 4H), 0.93 (t, J = 7.3 Hz, 3H). **^{13}C NMR** (75 MHz, DMSO): δ 170.6, 155.1, 136.4, 135.3, 127.7, 127.6, 127.2, 127.0, 127.0, 126.8, 65.4, 65.1, 53.7, 29.3, 28.3, 20.7, 17.5, 12.5. **HRMS** $[C_{27}H_{30}N_3O_4 + H]^+$ = 460.22249 found; 460.22308 calculated.

(1R,6S)-Cyclosulfate-5-*O*-(*tert*-butyl,but-3-ynyl)-phosphoryl-D-carba-ribofuranose (57).

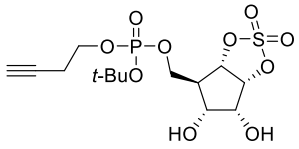

Compound **51α** (0.87 mg, 0.39 mmol) and DCI (68 mg, 0.58 mmol) were co-evaporated with anhydrous MeCN (3x) before dissolving in anhydrous MeCN (4.5 ml) and cooling to 0 °C. **56** (0.13 g, 0.46 mmol) was co-evaporated with toluene (2x), dissolved in anhydrous MeCN (1.5 ml) and added dropwise to the reaction mixture over a period of 10 min. Formation of the phosphotriester intermediate was monitored by ^{31}P NMR (δ = 136.7 ppm). After 75 min, *t*-BuOOH (5.5 M, 0.42 ml) was added in one go. The reaction mixture was stirred for 1.5 h at 0 °C, diluted with H_2O (30 ml) and brine (10 ml) and extracted with DCM (4x 30 ml). The combined organic fractions were dried over $MgSO_4$, filtered and concentrated under reduced pressure. Purification of the crude residue by silica gel column chromatography (DCM/acetone = 95:5 → 80:20) yielded title compound **57** (57 mg, 0.14 mmol, 36% over 2 steps) as a clear oil. **R_f** = 0.2 (DCM/actone = 70:30). **^{1}H NMR** (500 MHz, CD_3CN): δ 5.17 – 5.09 (m, 2H), 4.25 – 4.15 (m, 2H), 4.10 – 4.01 (m, 3H), 3.86 (dt, *J* = 8.6, 3.5 Hz, 1H), 3.05 (bs, 2H), 2.72 – 2.64 (m, 1H), 2.56 (td, *J* = 6.4, 2.7 Hz, 2H), 2.27 (t, *J* = 2.7 Hz, 1H), 1.48 (s, 9H). **^{13}C NMR** (126 MHz, CD_3CN): δ 84.8, 84.7, 84.4, 84.3, 84.3, 84.2, 83.1, 82.9, 81.3, 72.1, 72.0, 71.9, 71.6, 71.4, 66.2, 66.2, 65.7, 65.7, 65.6, 50.7, 50.7, 50.6, 30.0, 29.9, 21.0, 21.0. **^{31}P NMR** (202 MHz, CD_3CN): δ -4.68, -4.71. **HRMS** $[C_{14}H_{23}O_{10}PS + NH_4]^+$ = 432.10875 found, 432.10878 calculated; $[C_{14}H_{23}O_{10}PS + Na]^+$ = 437.06416 found, 437.06418 calculated.

(1R,6S)-Cyclosulfate-5-*O*-(but-3-ynyl)-phosphoryl-D-carba-ribofuranose (58).

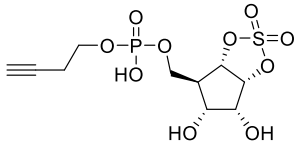

Compound **57** (25 mg, 0.060 mmol) and TIS (25 µl, 0.12 mmol) were dissolved in HCl (0.2 M in HFIP, 0.6 ml) in one go. After 1.5 h, the reaction mixture was diluted with toluene (10 ml) and concentrated under reduced pressure. The crude residue was dissolved in milliQ grade H_2O (10 ml) and washed with DCM (4x 5ml). The H_2O fraction was concentrated under reduced pressure and the residue was lyophilized to yield title compound **58** (13 mg, 0.035 mmol, 59%) as a clear oil. **^{1}H NMR** (300 MHz, DMSO): δ 5.43 – 5.25 (m, 2H), 4.34 (t, *J* = 4.2 Hz, 1H), 4.23 – 4.06 (m, 2H), 4.04 – 3.85 (m, 3H), 2.74 (d, *J* = 7.7 Hz, 1H), 2.54 (td, *J* = 6.3, 2.6 Hz, 2H), 2.38 (t, *J* = 2.6 Hz, 1H). **^{13}C NMR** (75 MHz, D_2O): δ 84.5, 82.9, 81.8, 70.9, 70.9, 70.5, 64.1, 64.0, 63.2, 63.1, 49.2, 49.1, 20.1, 20.0. **^{31}P NMR** (122 MHz, D_2O): δ 0.59. **HRMS** $[C_{10}H_{15}O_{10}PS + H]^+$ = 359.01933 found, 359.01963 calculated; $[C_{10}H_{15}O_{10}PS + Na]^+$ = 381.00138 found, 381.00157 calculated.

References

1. van der Heden van Noort, G. J. Chemical Tools to Study Protein ADP-Ribosylation. *ACS Omega* **5**, 1743–1751 (2020).
2. Liu, Q., Marel, G. A. van der & V. Filippov, D. Chemical ADP-ribosylation: mono-ADPr-peptides and oligo-ADP-ribose. *Org. Biomol. Chem.* **17**, 5460–5474 (2019).
3. Minnee, H. *et al.* Mimetics of ADP-Ribosylated Histidine through Copper(I)-Catalyzed Click Chemistry. *Org. Lett.* **24**, 3776–3780 (2022).
4. Boren, B. C. *et al.* Ruthenium-Catalyzed Azide−Alkyne Cycloaddition: Scope and Mechanism. *J. Am. Chem. Soc.* **130**, 8923–8930 (2008).
5. Gold, H. *et al.* Synthesis of Sugar Nucleotides by Application of Phosphoramidites. *J. Org. Chem.* **73**, 9458–9460 (2008).
6. Voorneveld, J. *et al.* Molecular Tools for the Study of ADP-Ribosylation: A Unified and Versatile Method to Synthesise Native Mono-ADP-Ribosylated Peptides. *Chem. Eur. J.* **27**, 10621–10627 (2021).
7. Mukaiyama, T. & Suda, S. Diphosphonium Salts as Effective Reagents for Stereoselective Synthesis of 1,2-cis-Ribofuranosides. *Chem. Lett.* **19**, 1143–1146 (1990).
8. van der Heden van Noort, G. J., Overkleeft, H. S., van der Marel, G. A. & Filippov, D. V. Ribosylation of Adenosine: An Orthogonally Protected Building Block for the Synthesis of ADP-Ribosyl Oligomers. *Org. Lett.* **13**, 2920–2923 (2011).
9. Li, Y. *et al.* Gold(I)-Catalyzed Glycosylation with Glycosyl ortho-Alkynylbenzoates as Donors: General Scope and Application in the Synthesis of a Cyclic Triterpene Saponin. *Chem. Eur. J.* **16**, 1871–1882 (2010).
10. Yu, B. Gold(I)-Catalyzed Glycosylation with Glycosyl o-Alkynylbenzoates as Donors. *Acc. Chem. Res.* **51**, 507–516 (2018).
11. Li, J. & Yu, B. A Modular Approach to the Total Synthesis of Tunicamycins. *Angew. Chem.* **127**, 6718–6721 (2015).
12. Kwon, Y., Schulthoff, S., Dao, Q. M., Wirtz, C. & Fürstner, A. Total Synthesis of Disciformycin A and B: Unusually Exigent Targets of Biological Significance. *Chem. Eur. J.* **24**, 109–114 (2018).
13. Nie, S., Li, W. & Yu, B. Total Synthesis of Nucleoside Antibiotic A201A. *J. Am. Chem. Soc.* **136**, 4157–4160 (2014).
14. Zhang, Q., Sun, J., Zhu, Y., Zhang, F. & Yu, B. An Efficient Approach to the Synthesis of Nucleosides: Gold(I)-Catalyzed N-Glycosylation of Pyrimidines and Purines with Glycosyl ortho-Alkynyl Benzoates. *Angew. Chem., Int. Ed.* **21**, 4933–4936 (2011).
15. Li, Y. *et al.* Synthesis of Kaempferol 3-O-[2′′,3′′- and 2′′,4′′-Di-O-(E)-p-coumaroyl]-α-l-rhamnopyranosides. *Synlett* **2011**, 915–918 (2011).
16. Mézailles, N., Ricard, L. & Gagosz, F. Phosphine Gold(I) Bis-(trifluoromethanesulfonyl)imidate Complexes as New Highly Efficient and Air-Stable Catalysts for the Cycloisomerization of Enynes. *Org. Lett.* **7**, 4133–4136 (2005).
17. Robinson, E. A., Henriksen, O. & Maxwell, E. S. Elongation Factor 2 AMINO ACID SEQUENCE AT THE SITE OF ADENOSINE DIPHOSPHATE RIBOSYLATION. *J. Biol. Chem.* **249**, 5088–5093 (1974).
18. Ness, B. G. V., Howard, J. B. & Bodley, J. W. ADP-ribosylation of elongation factor 2 by diphtheria toxin. NMR spectra and proposed structures of ribosyl-diphthamide and its hydrolysis products. *J. Biol. Chem.* **255**, 10710–10716 (1980).
19. Schaffrath, R., Abdel-Fattah, W., Klassen, R. & Stark, M. J. R. The diphthamide modification pathway from Saccharomyces cerevisiae – revisited. *Mol. Microbiol.* **94**, 1213–1226 (2014).
20. Su, X., Lin, Z. & Lin, H. The biosynthesis and biological function of diphthamide. *Crit. Rev. Biochem. Mol. Biol.* **48**, 515–521 (2013).
21. Honjo, T., Nishizuka, Y., Hayaishi, O. & Kato, I. Diphtheria Toxin-dependent Adenosine Diphosphate Ribosylation of Aminoacyl Transferase II and Inhibition of Protein Synthesis. *J. Biol. Chem.* **243**, 3553–3555 (1968).
22. Oppenheimer, N. J. & Bodley, J. W. Diphtheria toxin. Site and configuration of ADP-ribosylation of diphthamide in elongation factor 2. *J. Biol. Chem.* **256**, 8579–8581 (1981).
23. Evans, D. A. & Lundy, K. M. Synthesis of diphthamide: the target of diphtheria toxin catalyzed ADP-ribosylation in protein synthesis elongation factor 2. *J. Am. Chem. Soc.* **114**, 1495–1496 (1992).
24. Evans, D. A. & Bach, T. Selective Pd0-Mediated C‧ C Bond Constructions on the Imidazole Ring of L-Histidine: A Practical Approach to the Synthesis of Diphthamide and Related Histidine Analogues. *Angew. Chem., Int. Ed. Engl.* **32**, 1326–1327 (1993).
25. Van Ness, B. G., Howard, J. B. & Bodley, J. W. Isolation and properties of the trypsin-derived ADP-ribosyl peptide from diphtheria toxin-modified yeast elongation factor 2. *J. Biol. Chem.* **253**, 8687–8690 (1978).
26. Shimada, N. *et al.* Direct Synthesis of N-Protected Serine- and Threonine-Derived Weinreb Amides via Diboronic Acid Anhydride-Catalyzed Dehydrative Amidation: Application to the Concise Synthesis of -Garner's Aldehyde. *Synlett* **32**, 1024–1028 (2021).
27. Meffre, P., Hermann, S., Durand, P., Reginato, G. & Riu, A. Practical one-step synthesis of ethynylglycine synthon from Garner's aldehyde. *Tetrahedron* **58**, 5159–5162 (2002).
28. Jain, R., Avramovitch, B. & Cohen, L. A. Synthesis of ring-halogenated histidines and histamines. *Tetrahedron* **54**, 3235–3242 (1998).
29. Atsumi, S. *et al.* PRODUCTION, ISOLATION AND STRUCTURE DETERMINATION OF A NOVEL β-GLUCOSIDASE INHIBITOR, CYCLOPHELLITOL, FROM PHELLINUS SP. *J. Antibiot.* **43**, 49–53 (1990).
30. Schröder, S. P. *et al.* A Divergent Synthesis of l-arabino- and d-xylo-Configured Cyclophellitol Epoxides and Aziridines. *Eur. J. Org. Chem.* **2016**, 4787–4794 (2016).

31. Artola, M. *et al.* 1,6-Cyclophellitol Cyclosulfates: A New Class of Irreversible Glycosidase Inhibitor. *ACS Cent. Sci.* **3**, 784–793 (2017).
32. McGregor, N. G. S. *et al.* Rational Design of Mechanism-Based Inhibitors and Activity-Based Probes for the Identification of Retaining α-l-Arabinofuranosidases. *J. Am. Chem. Soc.* **142**, 4648–4662 (2020).
33. McGregor, N. G. S. *et al.* Cysteine Nucleophiles in Glycosidase Catalysis: Application of a Covalent β-l-Arabinofuranosidase Inhibitor. *Angew. Chem.* **133**, 5818–5822 (2021).
34. Deaglio, S. *et al.* Human CD38 (ADP-Ribosyl Cyclase) Is a Counter-Receptor of CD31, an Ig Superfamily Member. *J. Immun.* **160**, 395–402 (1998).
35. Zocchi, E. *et al.* A Single Protein Immunologically Identified as CD38 Displays NAD+ Glycohydrolase, ADP-Ribosyl Cyclase and Cyclic ADP-Ribose Hydrolase Activities at the Outer Surface of Human Erythrocytes. *Biochem. Biophys. Res. Commun.* **196**, 1459–1465 (1993).
36. Aarhus, R., Graeff, R. M., Dickey, D. M., Walseth, T. F. & Hon, C. L. ADP-ribosyl Cyclase and CD38 Catalyze the Synthesis of a Calcium-mobilizing Metabolite from NADP+. *J. Biol. Chem.* **270**, 30327–30333 (1995).
37. Liu, Q. *et al.* Structural Basis for the Mechanistic Understanding of Human CD38-controlled Multiple Catalysis. *J. Biol. Chem.* **281**, 32861–32869 (2006).
38. Liu, Q. *et al.* Covalent and Noncovalent Intermediates of an NAD Utilizing Enzyme, Human CD38. *Chemistry & Biology* **15**, 1068–1078 (2008).
39. Chen, Z. *et al.* Studies of the Synthesis of Nicotinamide Nucleoside and Nucleotide Analogues and Their Inhibitions Towards CD38 NADase. *ChemInform* **43**, (2012).
40. Wang, S. *et al.* Design, Synthesis and SAR Studies of NAD Analogues as Potent Inhibitors towards CD38 NADase. *Molecules* **19**, 15754–15767 (2014).
41. Shrimp, J. H. *et al.* Revealing CD38 Cellular Localization Using a Cell Permeable, Mechanism-Based Fluorescent Small-Molecule Probe. *J. Am. Chem. Soc.* **136**, 5656–5663 (2014).
42. Drach, J., Zhao, S. R., Malavasi, F. & Mehta, K. Rapid Induction of CD38 Antigen on Myeloid Leukemia Cells by All trans-Retinoic Acid. *Biochem. Biophys. Res. Commun.* **195**, 545–550 (1993).
43. Drach, J. *et al.* Retinoic Acid-induced Expression of CD38 Antigen in Myeloid Cells Is Mediated through Retinoic Acid Receptor-α. *Cancer Res* **54**, 1746–1752 (1994).
44. Volbeda, A. G. *et al.* Chemoselective Cleavage of p-Methoxybenzyl and 2-Naphthylmethyl Ethers Using a Catalytic Amount of HCl in Hexafluoro-2-propanol. *J. Org. Chem.* **80**, 8796–8806 (2015).
45. Tanaka, H., Yoshimura, Y., Jørgensen, M. R., Cuesta-Seijo, J. A. & Hindsgaul, O. A Simple Synthesis of Sugar Nucleoside Diphosphates by Chemical Coupling in Water. *Angew. Chem.* **124**, 11699–11702 (2012).
46. Wan, Z.-K., Binnun, E., Wilson, D. P. & Lee, J. A Highly Facile and Efficient One-Step Synthesis of N6-Adenosine and N6-2\`-Deoxyadenosine Derivatives. *Org. Lett.* **7**, 5877–5880 (2005).
47. Atdjian, C., Coelho, D., Iannazzo, L., Ethève-Quelquejeu, M. & Braud, E. Synthesis of Triazole-Linked SAM-Adenosine Conjugates: Functionalization of Adenosine at N-1 or N-6 Position without Protecting Groups. *Molecules* **25**, 3241 (2020).
48. Wang, Y., Liu, Y., Lu, T., Gao, F. & Zhao, B. Synthesis and Properties of 3-Azido-2,2-bis(azidomethyl)propyl 2-Azidoacetate: A Potential Azido Ester Plasticizer. *ChemPlusChem* **84**, 107–111 (2019).